AERIAL IMAGE ENHANCEMENT BASED ON ESTIMATION OF ATMOSPHERIC EFFECTS

Yuzhong Shen and Srinivas K. Jakkula

Old Dominion University
Department of Electrical and Computer Engineering
Norfolk, VA 23529
{yshen,sjakk001}@odu.edu

ABSTRACT

Aerial images are used extensively in many trip and mapping software packages, such as Google Earth and Microsoft Virtual Earth. These software packages provide a wealth of geospatial information including transportation, terrain, places, etc. Among the issues in effective utilization of aerial images, color tone discrepancy is the inconsistency in brightness, saturation, or color balance between images representing adjacent areas, causing adjacent areas appear significantly different that would otherwise be similar. This paper proposes novel algorithms that can significantly eliminate or reduce color tone discrepancies of aerial images based on estimation of atmospheric effects. Two algorithms are proposed for estimating the parameters of the translucent layer modeling the atmosphere. Proposed algorithm I utilizes a cost function approach and is suitable for images that have overlapped areas, while proposed algorithm II is based on statistical estimation and is suitable for arbitrary images representing adjacent areas. Enhanced images are obtained by removing atmospheric effects in the target images. Presented results demonstrate the effectiveness of proposed algorithms.

Index Terms— Color match, image enhancement, aerial images

1. INTRODUCTION

The last few years have witnessed rapidly increasing uses of digital maps or other geo-spatial information in various professions and people's everyday life. High quality aerial images are needed to make correct interpretations or ensure satisfactory user experiences. However, aerial images differ significantly due to the variations in atmospheric clarity, atmospheric layer density, humidity, temperature, angle and intensity of the solar beam, and other conditions under which the aerial images are captured. Aerial images are captured from aircrafts, spacecrafts, or satellites, with operating altitudes ranging from hundreds of meters to hundreds of kilometers. The atmosphere enclosing Earth has profound effects upon aerial images since the light, or more generally, electromagnetic radiation, must pass through portion or all of atmosphere depending on image sensor's altitude. Scattering and absorption are the major interactions between solar energy and Earth atmosphere [1]. Scattering is the redirection of electromagnetic energy by particles in the atmosphere or by atmospheric gas molecules. Scattering causes the atmosphere to exhibit its own color. Absorption of radiation occurs when the atmosphere attenuates the transmission of radiation through the atmosphere . In this paper, the effects of scattering and absorption are simulated by modeling the atmosphere as a translucent layer which has its own color. We propose two algorithms for estimating the parameters of the translucent layer modeling the atmosphere for different types of images. Proposed algorithm I utilizes a cost function approach and is suitable for images that have overlapped areas, while proposed algorithm II is based on statistical estimation and is suitable for arbitrary images representing adjacent areas.

This work was supported by Virginia Modeling, Analysis, and Simulation Center (VMASC) at Old Dominion University, Norfolk, Virginia.

2. PROPOSED ALGORITHMS

2.1. Proposed Algorithm I: Optimized Cost Function

Consider two images: a reference image $\mathbf{I}_R$ and a target image $\mathbf{I}_T$. Assume the image $\mathbf{I}_R$ is captured under ideal conditions, for example, the atmospheric effects upon images captured by low-flying aircraft can be negligible. The image $\mathbf{I}_T$ is captured under different conditions and has a color tone that is different from that of the reference image $\mathbf{I}_R$. Both images $\mathbf{I}_R$ and $\mathbf{I}_T$ capture the same area. In practical applications, images $\mathbf{I}_R$ and $\mathbf{I}_T$ can be obtained from the overlapped areas in two adjacent aerial images. In the proposed approach, the atmosphere color caused by scattering is represented by $\mathbf{I}_A$, which is assumed constant over large areas. The attenuation caused by absorption is modeled by a parameter $\mathbf{c}$ which contains several components corresponding to various bandwidth of the light. We model the relationships among $\mathbf{I}_R$, $\mathbf{I}_T$, $\mathbf{I}_A$, and $\mathbf{c}$ using RGB color space as follows [2].

$$\begin{aligned} I_{T,r}(m,n) &= (1-c_r)I_{R,r}(m,n) + c_r I_{A,r}, \\ I_{T,g}(m,n) &= (1-c_g)I_{R,g}(m,n) + c_g I_{A,g}, \\ I_{T,b}(m,n) &= (1-c_b)I_{R,b}(m,n) + c_b I_{A,b}, \end{aligned} \tag{1}$$

for $1 \leq m \leq M, 1 \leq n \leq N$, where $M \times N$ is the image size and the subscripts r, g, and b represent the red, green, and blue components. In this paper, we use boldface fonts to represent vectors and regular fonts for scalars. To further simplify notation, we remove the subscripts representing color components in (1) to represent any of red, green, and blue components as follows,

$$I_T = (1-c)I_R + cI_A. \tag{2}$$

Thus each color component of the target image $\mathbf{I}_T$ is a weighted sum of the corresponding component of the reference image $\mathbf{I}_R$ and that of the atmosphere color $\mathbf{I}_A$, where the weights are related to the atmospheric attenuation parameter $\mathbf{c}$. Generally the system of equations in (1) is overdetermined and has no exact solution, because the number of equations ($M \times N \times 3$) is substantially greater than the number of unknowns, which is 6 ($I_{A,r}$, $I_{A,g}$, $I_{A,b}$, c_r, c_g, and c_b). These equations are used to form a cost function by using the Method of Least Squares. The cost function is a measure of color tone discrepancies between the reference image and the target image and can be formed as

$$\begin{aligned} &\mathcal{F}(\mathbf{c}, \mathbf{I}_A) = \mathcal{F}(c_r, c_g, c_b, I_{A,r}, I_{A,g}, I_{A,b}) \\ &= \sum_{m=1}^{M}\sum_{n=1}^{N}((1-c_r)I_{R,r}(m,n) + c_r I_{A,r} - I_{T,r}(m,n))^2 \\ &+ \sum_{m=1}^{M}\sum_{n=1}^{N}((1-c_g)I_{R,g}(m,n) + c_g I_{A,g} - I_{T,g}(m,n))^2 \\ &+ \sum_{m=1}^{M}\sum_{n=1}^{N}((1-c_b)I_{R,b}(m,n) + c_b I_{A,b} - I_{T,b}(m,n))^2. \end{aligned} \tag{3}$$

The cost function (3) is to be minimized to reduce the color tone discrepancy between the images. The cost function minimization is done using the Steepest Descent Method. Its partial derivatives with respect to I_A and c are

$$\begin{aligned} \frac{\partial \mathcal{F}(\mathbf{c}, \mathbf{I}_A)}{\partial c} &= 2\sum_{m=1}^{M}\sum_{n=1}^{N}((1-c)I_R(m,n) + cI_A \\ &\qquad -I_T(m,n))(I_A - I_R(m,n)), \\ \frac{\partial \mathcal{F}(\mathbf{c}, \mathbf{I}_A)}{\partial I_A} &= 2\sum_{m=1}^{M}\sum_{n=1}^{N}((1-c)I_R(m,n) + cI_A \\ &\qquad -I_T(m,n))c, \end{aligned} \tag{4}$$

where again, I_A, I_R, I_T, and c represent one component of $\mathbf{I}_A$, $\mathbf{I}_R$, $\mathbf{I}_T$, and $\mathbf{c}$, respectively. Then $\mathbf{I}_A$ and $\mathbf{c}$ can be solved iteratively using the Steepest Descent Method,

(a) (b)

Fig. 1. Images representing similar features

$$c_{i+1} = c_i - \mu_c \frac{\partial \mathcal{F}(\mathbf{c}_i, \mathbf{I}_{A,i})}{\partial c_i}, \tag{5}$$

$$I_{A,i+1} = I_{A,i} - \mu_{I_A} \frac{\partial \mathcal{F}(\mathbf{c}_i, \mathbf{I}_{A,i})}{\partial I_{A,i}}, \tag{6}$$

where i is the iteration number, μ_c and μ_{I_A} are the step sizes for c and I_A, respectively. After the values of $\mathbf{c}$ and $\mathbf{I}_A$ are computed, the enhanced image can be obtained by removing the atmospheric effects as follows,

$$I_E = (I_T - cI_A)/(1-c), \tag{7}$$

where I_E represents one color component of the enhanced image $\mathbf{I}_E$.

2.2. Proposed Algorithm II: Statistical Estimation

Unlike proposed algorithm I that requires the target image and the reference image have overlapped areas and the same resolution, proposed algorithm II works on arbitrary images representing adjacent areas even with different resolution. Proposed Algorithm II is based on the observation that, images representing similar features or objects, have similar statistical characteristics if they were captured under the same conditions [3]. The most commonly used statistical variables are mean, variance, and median. The two images in Fig. 1 represent similar features, i.e., both contain building, parking lot, bushes, etc. The mean, variance, and median of all pixel values of red, green, and blue color components of these two images are shown in Table 1. It is clear that these statistical characteristics of both images are very similar from Table 1. Proposed algorithm only utilizes mean and variance because they are simple to compute, while median can take significant amount of time.

Assume $\mathbf{I}_R$ and $\mathbf{I}_T$ are two sub-images representing similar features in the reference image and target image captured under different conditions. Since $\mathbf{I}_R$ and $\mathbf{I}_T$ represent similar features, they should have similar statistical characteristics if they were captured under the same conditions. Thus

Table 1. Image Statistical Characteristics

Color	Image	Mean	Variance	Median
Red	1(a)	131.66	2741.5	129
	1(b)	134.05	2533.1	137
Green	1(a)	138.46	2749.9	133
	1(b)	143.64	2606.1	147
Blue	1(a)	128.95	2524.0	122
	1(b)	132.07	2238.2	132

the enhanced image $\mathbf{I}_E$ from $\mathbf{I}_T$ should have similar statistic characteristics as $\mathbf{I}_R$. That is,

$$\begin{aligned} E(\mathbf{I}_R) &= E(\mathbf{I}_E), \\ \mathrm{var}(\mathbf{I}_R) &= \mathrm{var}(\mathbf{I}_E), \end{aligned} \tag{8}$$

where $E(\cdot)$ and $\mathrm{var}(\cdot)$ are the mean and variance of all the pixels in an image. By solving the system of equations in (8) we can obtain the exact solution for $\mathbf{I}_A$ and $\mathbf{c}$. The derivation of solving (8) for $\mathbf{I}_A$ and $\mathbf{c}$ is omitted in this paper as the space is limited. The solutions of $\mathbf{c}$ and $\mathbf{I}_A$ are

$$c = 1 - (MN\sum_{k=1}^{K}\sum_{l=1}^{L}(I_T(k,l) - \frac{1}{KL}\sum_{k=1}^{K}\sum_{l=1}^{L} I_T(k,l))^2)^{1/2} \\ /(KL\sum_{m=1}^{M}\sum_{n=1}^{N}(I_R(m,n) - \frac{1}{MN}\sum_{m=1}^{M}\sum_{n=1}^{N} I_R(m,n))^2)^{1/2}, \tag{9}$$

$$I_A = \frac{1}{cKL}\sum_{k=1}^{K}\sum_{l=1}^{L} I_T(k,l) - \frac{1-c}{cMN}\sum_{m=1}^{M}\sum_{n=1}^{N} I_R(m,n), \tag{10}$$

where $M \times N$ and $K \times L$ are the sizes of the reference image $\mathbf{I}_R$ and target image $\mathbf{I}_T$ respectively. Equations (9) and (10) represent a single color component in the RGB color space; thus they should be applied to red, green, and blue color components separately. After obtaining $\mathbf{I}_A$ and $\mathbf{c}$, the enhanced image $\mathbf{I}_E$ is computed using equation (7).

3. EXPERIMENTAL RESULTS

In this section, we present some experimental results of the proposed algorithms applied to various types of images. The images in Fig. 2 represent some urban residential areas and were captured under different conditions. The image shown in Fig. 2(a) is the reference image, while the image in Fig. 2(b) is the target image to be enhanced. The reference image and target image have different color tones and also have an overlapped area, indicated by the red rectangle in both images. Fig. 2(c) shows the enhanced image generated by algorithm I and it is clear that the enhanced image and the reference image in Fig. 2(a) have similar, if not identical, color tones.

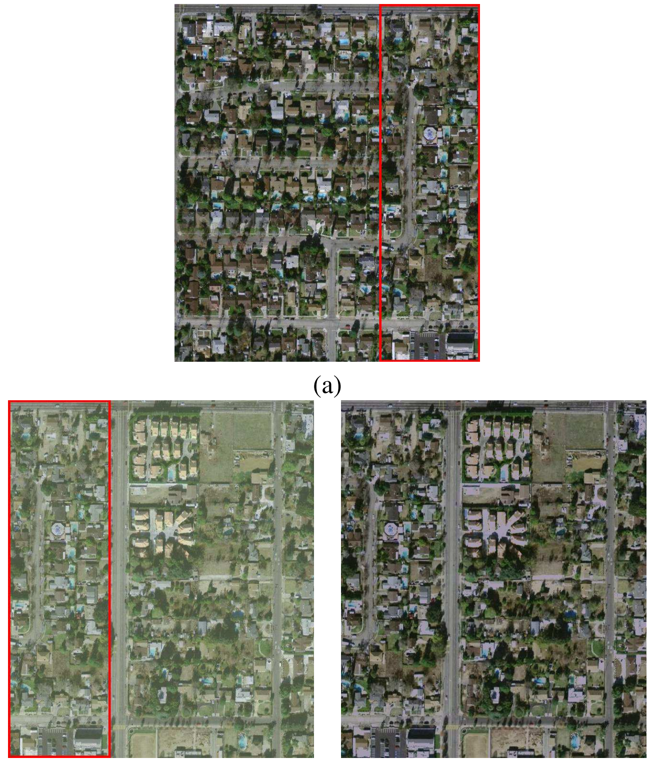

(a)

(b) (c)

Fig. 2. Proposed Algorithm I results. (a) The reference image, (b) the target image, and (c) the enhanced image generated from Algorithm I.

Fig. 3 shows the iterations of the Steepest Descent Method used by proposed algorithm I and it can be seen that both $\mathbf{c}$ and $\mathbf{I}_A$ converge after 1000 iterations, while the cost function shown in Fig. 3(c) reaches its minimum after 400 iterations. The results shown in Fig. 3 and Fig. 2 demonstrate the effectiveness of proposed algorithm I.

Fig. 4(a) shows another image, depicting an area with different color tones, where the left half image appears natural under normal conditions and the right half image does not. Also note that the left half image and right half image do not have overlapped regions. The left half image is taken as the reference image, and the right half image is taken as the target image. Algorithm II is used to enhance the target image (right half image), yielding the result image shown in Fig. 4(b). The color tone discrepancy in Fig. 4(a) is removed and the result image exhibits uniform color tone.

4. CONCLUSION

Two algorithms for estimation of atmospheric effects in aerial image enhancement have been proposed in this paper. The atmosphere is modeled as a translucent layer with its own color. Proposed algorithm I utilizes the cost function approach and

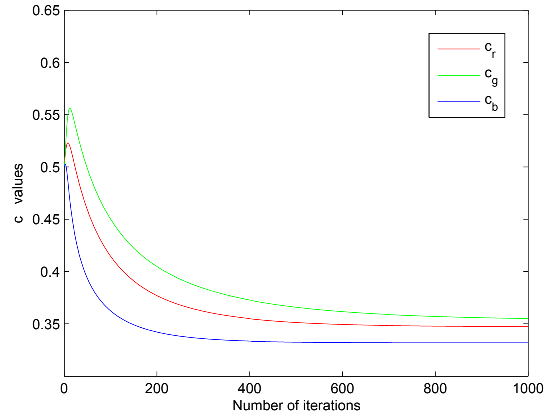

(a)

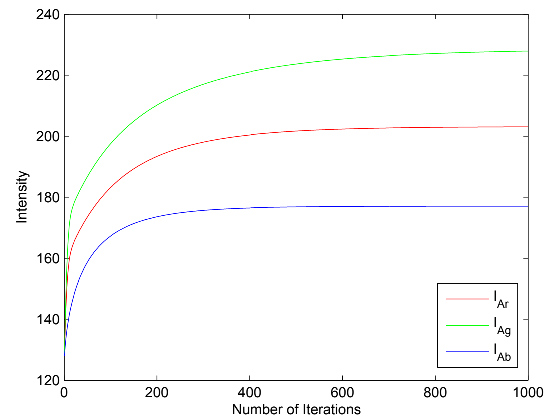

(b)

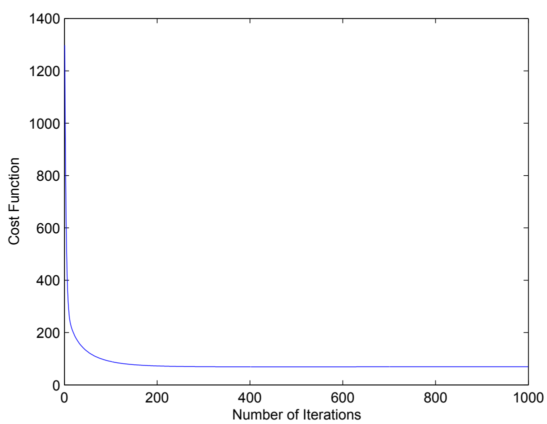

(c)

Fig. 3. Convergence of proposed algorithm I. (a) Convergence of transparency parameter $\mathbf{c}$. (b) Convergence of atmosphere layer $\mathbf{I}_A$. (c) Cost function normalized by image size.

(a)

(b)

Fig. 4. Proposed Algorithm II results: (a) The image with different color tones and (b) the uniform image generated form Algorithm II.

is suitable for images that have overlapped areas. Steepest descent Method is used for optimizing the cost function. Proposed algorithm II is based on statistical estimation and is suitable for arbitrary images representing adjacent areas. The images are then enhanced by removing atmospheric effects. Presented figures and graphs demonstrate the effectiveness of the proposed algorithms.

5. REFERENCES

[1] H. Fallah-Adl, J. Jaja, S. Liang, J. Townshend, and Y.J. Kaufman, "Fast algorithms for removing atmospheric effects from satellite images," in *IEEE Computational Sciences and Engineering*, Summer 1996, vol. 3 of *Issue 2*, pp. 66–77.

[2] Ming-Sui, Lee Meiyin Shen, and C. C. Jay Kuo, "Color matching techniques for video mosaic applications," in *IEEE International Conference on Multimedia and Expo*, June 2004, vol. 1, pp. 121–124.

[3] E. Reinhard, M. Adhikhmin, B. Gooch, and P. Shirley, "Color transfer between images," in *IEEE Computer Graphics and Applications*, July-Aug 2001, vol. 21 of *Issue 5*, pp. 34–41.